Received: 4 August 2023 | Revised: 21 September 2023 | Accepted: 29 September 2023

DOI: 10.1111/jfpe.14475

ORIGINAL ARTICLE

Journal of Food Process Engineering WILEY

Machine learning approaches for estimating apricot drying characteristics in various advanced and conventional dryers

Mohammad Kaveh[1] | Necati Çetin[2] | Esmail Khalife[3] | Yousef Abbaspour-Gilandeh[4] | Maryam Sabouri[5] | Faroogh Sharifian[6]

[1]Department of Petroleum Engineering, College of Engineering, Knowledge University, Erbil, Iraq

[2]Department of Agricultural Machinery and Technologies Engineering, Faculty of Agriculture, Ankara University, Ankara, Turkey

[3]Department of Civil Engineering, Cihan University-Erbil, Erbil, Iraq

[4]Department of Biosystems Engineering, College of Agriculture and Natural Resources, University of Mohaghegh Ardabili, Ardabil, Iran

[5]Scientific Research Center, Erbil Polytechnic University, Erbil, Iraq

[6]Department of Mechanical Engineering of Biosystems, Faculty of Agriculture, Urmia University, Urmia, Iran

Correspondence
Necati Çetin, Department of Agricultural Machinery and Technologies Engineering, Faculty of Agriculture, Ankara University, Ankara, Turkey.
Email: necati.cetin@ankara.edu.tr

Abstract

Drying plays a crucial role in preserving the quality of agricultural products. Nevertheless, suboptimal conditions in drying systems have an adverse effect on drying characteristics and energy efficiency. Machine learning approaches are innovative and reliable that have been successfully used to solve such challenges and achieve optimization in drying processes. In this study, five machine learning approaches (multilayer perceptron [MLP], gaussian processes [GP], support vector regression [SVR], k-nearest neighbors [kN], and random forest [RF]) were used to estimate moisture content and moisture ratio of apricot in five various dryers (convective [CV], microwave [MW], infrared [IR], microwave-convective [MW-CV], and infrared-convective [IR-CV]). Also, the values of specific energy consumption (SEC) and effective moisture diffusivity (D_{eff}) were calculated in these dryers. Accordingly, the best result of the D_{eff} (3.14×10^{-10} m^2/s) and the minimum value of the drying time (130 min) and SEC (18.67 MJ/kg) were obtained using MW-CV hybrid dryer. While the lowest values of D_{eff} (2.09×10^{-11} m^2/s) and highest drying time (18.5 h) and SEC (209.34 MJ/kg) were detected in CV dryer at 50°C. The best correlation coefficients (R) for the estimation of moisture content were gained using RF technique for k-fold cross validation and train-test split with the values of 0.9908 and 0.9912, respectively. Moreover, moisture ratio results showed that the MLP achieved the highest R value over 0.9985 for both validation methodologies. In the discrimination of the drying methods, the MLP had the greatest accuracy as 82.00% and 86.00% for k-fold cross validation and train-test split, respectively. The results showed that the RF and ML models could potentially be used for estimation and discrimination for drying applications.

Practical Applications

Recently, there has been an increased interest in healthy food choices such as foodstuffs, snacks, and dried products. This trend has captured the attention of both

Abbreviations: ANN, artificial neural networks; AOAC, Association of Official Agricultural Chemists; CV, convective; d.b., dry basis; D_{eff}, effective moisture diffusivity; DT, decision tree; EMD, effective moisture diffusion; FN, false negative; FP, false positive; GP, Gaussian processes; IR, infrared; IR-CV, infrared-convective; IR-CV-R, infrared-convective-rotary; KNN, k-nearest neighbors; MAE, mean absolute error; MC, moisture content; MCC, Matthew's correlation coefficient; MJ, megajoule; ML, machine learning; MLP, multilayer perceptron; MR, moisture ratio; MW, microwave; MW-CV, microwave-convective; MW-CV-R, microwave-convective-rotary; PRC, precision–recall; PUK, Pearson VII Kernel function; R, correlation coefficient; R^2, determination coefficient; RAE, relative absolute error; RF, random forest; RMSE, root mean square error; ROC, receiver operating characteristic; RRSE, root relative squared error; SEC, specific energy consumption; SVR, support vector regression; TN, true negative; TP, true positive.

dietitians and conscious consumers. Apricots are a prime example of a valuable dried product that can be dry in various conditions. Machine learning techniques can be used for rapid and non-destructive determination of drying characteristics and such techniques yield objective and accurate results. Present findings revealed that texture machine learning models could be used as an effective and reliable discrimination tool for dried products.

KEYWORDS
apricot, drying, estimation, machine learning, moisture

1 | INTRODUCTION

Evaluation of a drying device from the point view of design, energy, and storage properties as well as material transfer for agriculture products passes through the drying kinetics evaluation (Rodríguez et al., 2014). Several numerical methods like mathematical modeling and response surface methodology have managed to resolve the complexity of nonlinear behavior up to a point. To overcome the drawbacks of these methods, some different techniques like artificial neural network (ANN), fuzzy logic, and logistic regression have been considered (Abbasi et al., 2010). Some of these techniques are k-nearest neighbor (k-NN), support vector machine (SVM), Gaussian processes (GP), random forest (RF), and multilayer perceptron (MLP) (Rodríguez et al., 2014). These algorithms are a potential tool for simulating drying process variables and tackle the complexity of the nonlinear systems (Bahmani et al., 2016; Guiné et al., 2014). Mathematical modeling is a very complex and time-consuming procedure for estimating mass characteristics based on input effects. For this reason, machine learning technique are preferred over mathematical modeling due to the logical precision and low computation times in the drying process (Afkhamipour et al., 2018).

Machine learning algorithms provide a substitute method for solving problems and their use is increasing day by day. The ability to tune multinomial nonlinear functions was the main reason for successful use of these algorithms (Golpour et al., 2018; Silva et al., 2015). These algorithms have been often used to imitate and modeling the behavior of agriculture products (Golpour et al., 2020). In addition, ML method offers some benefits over traditional statistical and mathematical procedures. In better word, they do not require the estimated values be placed around the mean and thus imitate actual values variability (Jahanbakhshi & Salehi, 2019; Movagharnejad & Nikzad, 2007; Shekarchizadeh et al., 2014).

The main key variables in the drying process are moisture ratio, moisture content, and drying rate. A few investigations have considered the drying characteristics estimation using machine learning approaches including for pineapple cubes (Meerasri & Sothornvit, 2022), apple slices (Sağlam & Çetin, 2022), pomelo fruit (Kırbaş et al., 2019), mushroom (Tarafdar et al., 2019), cocoyam slices (Onu et al., 2022), apricot slices (Satorabi et al., 2021), orange slices (Çetin, 2022a), orange-fleshed sweet potato (Okonkwo et al., 2022), banana (Trivedi et al., 2023), cantaloupe (Zadhossein et al., 2023). In addition, there are rare discrimination research about drying of agriculture product in the past studies such as dried strawberry (Przybył et al., 2020), freeze-dried beetroot (Ropelewska & Wrzodak, 2022), dried tarhana (Kurtulmuş et al., 2014), and dried garlic (Makarichian et al., 2021). These studies disclose that there are limited available research about the modeling machine learning based of drying parameters particularly moisture content and moisture ratio estimation of apricot. Moreover, there is no study on discrimination of the drying methods according to such drying characteristics, to the best of found knowledge. The innovative aspect of this study is related to the modeling of moisture content and moisture content models in apricot drying processes with five different machine algorithms instead of conventional mathematical methods and comparative analysis of the performance results obtained. In addition, another difference in the study is that three different machine learning algorithms perform classification according to apricot drying conditions. The current investigation is the first work to estimate and analyze the moisture content and moisture ratio and the drying methods comparing using above-mentioned drying characteristics.

2 | MATERIALS AND METHODS

2.1 | Sample preparation

The present research was performed in 2022 in the Department of Biosystem Engineering, at Mohaghegh Ardabili University in Iran. The apricot samples were prepared from a local garden (Sardasht, Iran) and were kept in a refrigerator (3°C) until the end of the tests. About 60 min before the start of each test, the samples were adapted to ambient temperature to balance the temperature by removing from the refrigerator. The preliminary moisture content of apricot samples was measured based on AOAC standard (AOAC, 1990). The process continued until the weight of the samples was fixed. The samples were removed from the oven and their weight was immediately measured and weighed, then the initial moisture content of apricot was obtained on a dry basis according to Equation (1) (Kayran & Doymaz, 2021). A scale was used to record the weight of the samples with a resolution of 0.001 g (AND model GF-6000, Japan). The primary moisture content was 4.95 ± 0.72 kg water per kg on dry basis (d.b.) (Shimpy & Kumar, 2023).

$$MC_{d.b} = \frac{W_0 - W_d}{W_d} \times 100 \quad (1)$$

where W_0 stands for the initial weight, W_d refers for the weight of the dried product, and $MC_{d.b.}$ refers for the moisture content percentage on d.b.

2.2 | Drying technologies

Drying processes were done in a hybrid dryer (microwave-convective-rotary [MW-CV-R]) and (infrared-convective-rotary [IR-CV-R]) in the laboratory of the above-mentioned department (the rotary part was removed to perform the tests of this study) (Kaveh & Abbaspour-Gilandeh, 2019; Kaveh & Abbaspour-Gilandeh, 2022). Hybrid dryers (MW-HA-R and IR-HA-R) can use convection (CV), microwave (MW), and infrared (IR) methods separately and combined together (MW-CV and IR-CV). Three thermal elements (4.8 kW) were used to measure air temperature in these dryers. Hot air was blown into the chamber by a blower (1 hp/3000 rpm). The temperature of the air blown was controlled by a thermostat. The air velocity for all tests of the CV dryer was determined 0.5 m/s individually and in combination with MW and IR. In addition, four IR lamps (1000 W) were used inside the dryer. A 15 cm distance was chosen between the IR-lamps and the apricot sample. Two magnetrons (with a total power of 900 W) were used in the MW dryer and MW-CV combination. All required drying characteristics such as the sample mass, the inlet air temperature (K-type sensor throughout the dryer), the sample temperature, the ambient temperature, the ambient humidity (thermometer, Lutron TM-903, Taiwan), air velocity (anemometer, Lutron AM-4216, Taiwan), MW power, and IR power were continuously recorded on a personal computer equipped with data collection software. Different air temperature, microwave power, and infrared power levels for all employed dryers are presented in Table 1. The apricot samples were sliced in 3 mm by a fruit slicer for drying experiments. The amount of sample for drying tests for all dryers was about 80 ± 3 g and all the tests were done in three repetitions.

2.3 | Moisture ratio

According to the experimental data obtained from the tests and monitoring of the drying process, the moisture ratio parameter (without dimension during drying) of the apricot samples was obtained from Equation (2) (Tripathy & Srivastav, 2023):

$$MR = \frac{M_t - M_e}{M_O - M_e} \quad (2)$$

where M_t is the moisture content of the apricot sample at any moment (d.b), M_e stands for the equilibrium moisture content of the apricot sample (d.b), and M_0 refers to the primary moisture content of the sample (d.b). The amount of M_e compared to the values M_0 and M_t are very small if the drying time is prolonged (Polat & Izli, 2022). Therefore, the equation of MR during drying can be written as Equation (3), and there is no need to measure the equilibrium moisture to calculate the MR (Kayran & Doymaz, 2019).

$$MR = \frac{M_t}{M_O} \quad (3)$$

2.4 | Effective moisture diffusivity

The D_{eff} is a key feature for demonstrating the rate of moisture flow inside the sample, which indicates the difficulty of passing moisture from the inner parts of the sample to the outside. Fick's second law is explicated as the following equation. This law assumes the 1-D flow of moisture and the constant effective moisture penetration coefficient (Bao et al., 2023).

$$\frac{\partial M}{\partial t} = D_{eff} \frac{\partial^2 M}{\partial x^2} \quad (4)$$

The general solution of Fick's second law in Cartesian coordinates is expressed by Crank for a blade-shaped body as follows (Souza et al., 2022):

$$MR = \frac{M_t - M_e}{M_o - M_e} = \frac{8}{\pi^2} \sum_{n=1}^{\infty} \frac{1}{(2n+1)} \exp\left(-(2n+1)^2 \frac{D_{eff}}{4L^2} \pi^2 t\right) \quad (5)$$

where t refers to the drying time (s), D_{eff} refers to the effective moisture diffusivity (m^2/s), and L stands for the half thickness of the cut pieces of apricot (m^2). If the drying time is prolonged, Equation (5) can be shown as follow and just the first term of the equation be considered (Chikpah et al., 2022):

$$MR = \frac{8}{\pi^2} \exp\left(\frac{-D_{eff} \pi^2}{4L^2} t\right) \quad (6)$$

Now, the D_{eff} can be obtained from the slope method. Accordingly, the logarithm value of the moisture ratio obtained of the dried

TABLE 1 Stages of drying processes for drying apricot.

Process	CV	IR	MW	IR-CV	MW-CV
Air temperature (°C)	50 and 70	–	–	60	60
Infrared power (W)	–	500 and 750	–	500	–
Microwave power	–	–	360 and 630	–	540

Abbreviations: CV, convective; IR, infrared; MW, microwave.

samples against time gives a linear equation of K slope (Namjoo et al., 2022).

$$\ln(\mathrm{MR}) = \ln\frac{8}{\pi^2} - \frac{-D_{\mathrm{eff}}\pi^2}{4L^2}t \tag{7}$$

$$K = \left(\frac{D_{\mathrm{eff}}\pi^2}{4L^2}\right) \tag{8}$$

2.5 | Specific energy consumption

Specific energy consumption (SEC) during the drying of apricot samples using convective (E_{CV}), microwave (E_{MW}), and infrared (E_{IR}) methods were obtained from Equations (9)–(11), respectively as following (Kaveh et al., 2023; Motevali et al., 2011):

$$E_{CV} = \frac{A\,v\,\rho_a\,C_a\,\Delta t\,t}{M_w} \tag{9}$$

$$E_{MW} = \frac{P_{MW}\,t}{M_w} \tag{10}$$

$$E_{IR} = \frac{K\,t}{M_w} \tag{11}$$

where E_{CV}, E_{MW}, and E_{IR} are the SEC in convective, microwave and infrared dryer (MJ/kg), respectively, A is the apricot sample tray area (m^2), ρ_a is the air density (kg/m^3), ΔT is the temperature difference (°C), v refers to the air flow velocity (m/s), C_a refers to the air specific heat (kJ/kg°C), t refers to the period of drying (h), P_{MW} and K refer to the microwave and infrared power, respectively.

Energy consumption in microwave-convective ($E_{MW\text{-}CV}$) and infrared-convective ($E_{IR\text{-}CV}$) methods was obtained from the following Equations (12) and (13), respectively (EL-Mesery & El-khawaga, 2022).

$$E_{MW-CV} = eq_9 + eq_{10} \tag{12}$$

$$E_{IR-CV} = eq_9 + eq_{11} \tag{13}$$

where E_{MW-CV} and E_{IR-CV} are the SEC in microwave-convective and infrared-convective dryers (MJ/kg), respectively.

2.6 | Machine learning approaches

In the present research, a modeling and discrimination evaluation of developed algorithms were performed by the Weka® v3.8 software (Hall et al., 2009). Models were carried out on a personal computer. In this study, five different approaches (MLP, GP, support vector regression (SVR), KNN, and RF) were employed for parameter estimation. These algorithms provide very successful results for drying characteristics that occur in non-linear complex drying processes. In some studies, similar models were developed and performed well in drying processes (Çetin, 2022a; Sağlam & Çetin, 2022). Four characteristics including drying methods, drying time, moisture content (dry basis), and drying rate were used as the inputs for estimation the moisture ratio, and three characteristics (drying method, drying time, and drying rate) were employed as input for estimation the moisture content.

The discrimination of drying methods by three machine learning algorithms (MLP, RF, and KNN) were based on the drying characteristics as drying time, MC (dry basis), MR, drying rate, and ln (MR). In the present study, a number of 271 values were employed for each characteristic and the total sample size was 1626.

2.6.1 | Multilayer perceptron

The strength ANNs is in imitating the human brain behavior. ANN is a system including relationships between elements similar to biological neurons, and each of which has its specific weight (Loan et al., 2023). One of the widely used structures is MLP which is used for various aims such as classification and regression (Daliran et al., 2023). Three layers of input, hidden and output form MLPs structure. In addition, the data in this neural network flows from the input side to the output side, which is called feedforward neural network. The type of MLP training algorithm is backward propagation of errors which has been designed to analyze the weighted sum of the activation function (Çetin et al., 2021; Malakar et al., 2023). In the MLP, the number of neurons in the hidden layer is generally determined using a trial-and-error procedure (Bateni et al., 2007). In the MLP, it is recommended to choose the number of neurons in the hidden layer more than two times the input parameters (Varol et al., 2022). These criteria were considered when creating ANN architectures and the structures that give the most successful results at the end of the trials were preferred. For the development of ANN structure for moisture content, the structures of developed ANN were 3-3-1, 3-6-1, and 3-9-1, respectively. The three structures for estimation of moisture ratio were 4-4-1, 4-8-1, and 4-12-1, respectively. For all MLP structures, the number of epochs was 500, learning ratio was 0.3, the momentum coefficient was 0.2, and the Sigmoid was chosen as the activation function. Figure 1 depicts the applied MLP model structure. Furthermore, a specific MLP structure was developed for moisture ratio and moisture content.

2.6.2 | Gaussian processes

Gaussian process is a collection of random variables that set a joint Gaussian distribution (Rasmussen & Williams, 2006). In the GP model, the Bayesian Gaussian method as infinite dimensional parameter was employed for non-linear regression functions. It also needs defining a kernel function with a noise assessing capability or goodness of fit. In addition, to increase the performance of the developed model, the normalized and standardized data are used as the input values of the training step (Çetin, 2022b). The importance of this process is due to the fact all the employed features are obtained from the normal distribution, the normal distribution of error, variance, and covariance (Rasmussen & Williams, 2006). Current research, has used Pearson VII as the kernel function of the GP.

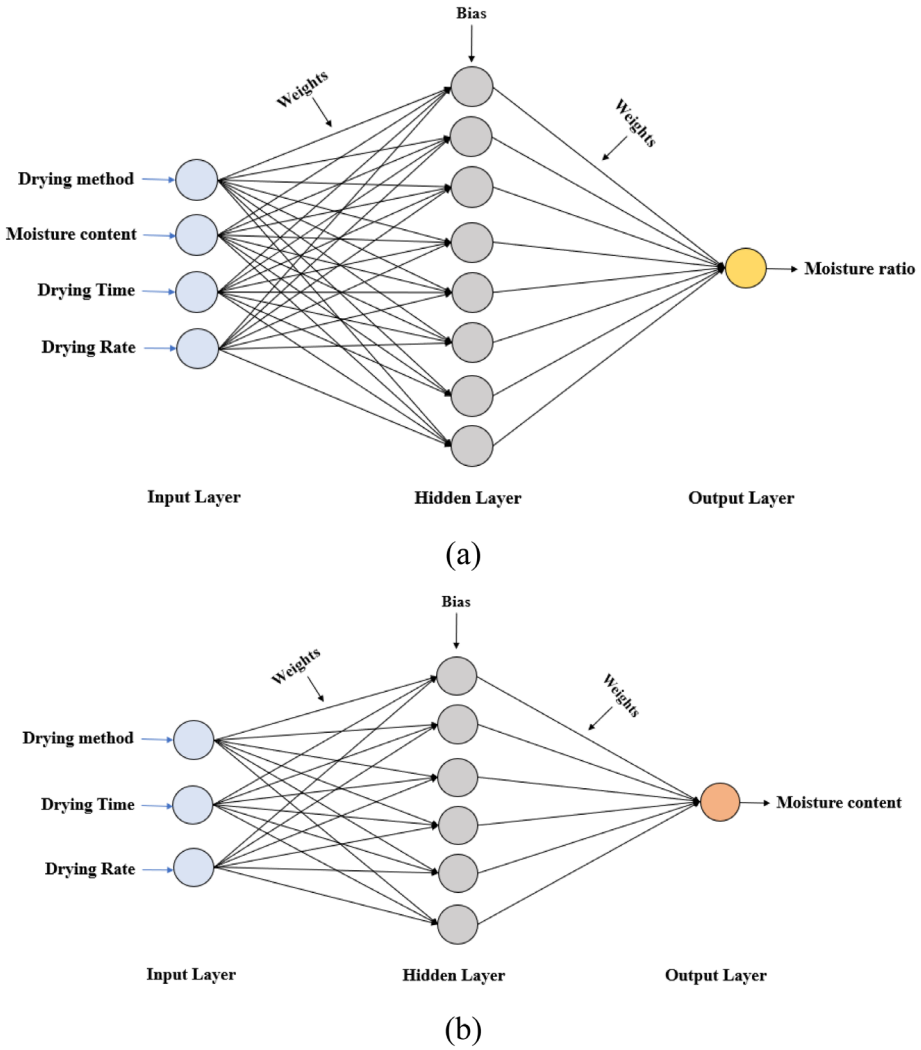

FIGURE 1 Representative multilayer perceptron model structures for moisture ratio (a) and moisture content (b).

2.6.3 | Support vector regression

Support vector regression is well known kind of machine learning frequently have been used for regression problems. SVR has core-oriented functionality and the features of kernel used have a significant impact on optimal development (Zhang et al., 2022). The results of using this technique on nonlinear problems have been very impressive. In SVR, the input variables are nonlinearly mapped in a feature space using kernel transformation function. To implement the process, the inputs and outputs values relationship is linearized in the feature space (Luka et al., 2022). Equation (14) illustrates the general state of SVR equation:

$$y = w\Phi(x) + b \ \ (\Phi : R_n \rightarrow R_N) \tag{14}$$

$x \in R_n$ refers to the input value, $y \in R_N$ refers to the output, b refers to the bias term, $w \in R_N$ refers to the coefficient factor, and Φ refers to the mapping function whose input is transformed into a high-dimensional vector. As mentioned in the last subsection, the selected SVR was Pearson VII (PUK) as kernel function.

2.6.4 | k-Nearest neighbor

Another powerful algorithm which has been used for different classification purposes especially in agriculture domain is k-NN. This algorithm the input values are categorized into some clusters and subsequently they will be combined and converted into new clusters. To calculate the distance, the well-known method of the Euclidean distance formula was used (Peter et al., 2021; Romero et al., 2013). In algorithm k-NN, there is no a training model for the structure, therefore, the performance of the system increases by increasing the number of learning samples (Maxwell et al., 2018). In addition, Euclidean distance was employed for searching process in k-NN algorithm, and k values for estimation and discrimination were 1, 3, and 5; and 3, respectively.

2.6.5 | Random forest

To build the RF classifier, first several decision trees are developed with self-learning examples with the actual training input values to develop each tree in regression. Afterwards, all the decision trees are

employed to estimate a specific model based on the convergent estimation model of all the models. Based on the fact, each decision tree is a unique model in RF, this convergent estimation is an instance of characteristic estimation (Breiman, 2001). Contrary to DT, the allotted class of data groups is determined by the most frequent of the groups of trees developed by RF (Berhane et al., 2018). Another advantage of this method is that the self-learning and ensemble scheme controls the overfitting weakness by DT, there is no pruning phase in RF (Ali et al., 2012). Moreover, RF could provide a more accurate model and has higher adaptability data fluctuations (Breiman, 2001; Rodriguez-Galiano et al., 2012).

2.7 | Validation methodology

The data was divided into two parts train set group (70%) and test part data (30%). In addition, k-fold cross validation approach was employed for validation phase (Sağlam & Çetin, 2022). Similar trend was followed for the discrimination. The performance of the models was assessed using a validation set in order to generate sufficient data for the training set. For this reason, 10-fold cross-validation was included to adjust the model hyperparameters. Generally, the greater the number of iterations, the greater the performance accuracy. However, the accuracy of network recognition does not improve and occasionally even declines after a certain number of epochs (Ashtiani et al., 2021; Wu et al., 2020). For all the models, *k* value was 10. The number of iterations for the training and testing procedures was 10. In each iteration, one sub-set was employed for testing and the rest sub-sets (9) were employed for training. Each *k* sub-samples were used once for testing. Afterwards, the overall error of the model was obtained using the average errors obtained in each iteration (Çetin, 2022b). Finally, the operational accuracy of the classifiers was evaluated by using specified performance parameters.

2.8 | Evaluation of model performances

Some statistical criteria such as correlation coefficient (*R*), mean absolute error (MAE), root mean square error (RMSE), relative absolute error (RAE), and root relative squared error (RRSE) were employed to evaluate the performance of the models (Equations 15–19) (Parker, 2001). Equations (20)–(23) were used to calculate the parameters of true positive (TP) rate, precision, F-measure, Matthew's correlation coefficient (MCC), receiver operating characteristic (ROC) area, and Precision–Recall (PRC) area for discrimination were calculated using (Ropelewska & Szwejda-Grzybowska, 2021). The MCC produces a high value only if the classifier correctly estimated most of the positive data instances and most of the negative data instances, and if most of its positive estimation and most of its negative estimations are correct (worst value = −1; best value = +1) (Chicco et al., 2021).

$$R = \frac{1}{n-1}\sum_{i=1}^{n}\frac{\left(M_i - \dot{M}\right)\left(E_i - \dot{E}\right)}{S_M\, S_E} \tag{15}$$

$$\mathrm{MAE} = \sum_{i=1}^{n}\frac{|E_i - M_i|}{n} \tag{16}$$

$$\mathrm{RMSE} = \sqrt{\frac{\sum_{i=1}^{n}(E_i - M_i)^2}{n}} \tag{17}$$

$$\mathrm{RAE} = \frac{\sum_{i=1}^{n}|E_i - M_i|}{\sum_{i=1}^{n}|\dot{M} - M_i|} \times 100 \tag{18}$$

$$\mathrm{RRSE} = \sqrt{\frac{\sum_{i=1}^{n}(E_i - M_i)^2}{\sum_{i=1}^{n}\left(\dot{M} - M_i\right)^2}} \times 100 \tag{19}$$

$$A_c = \frac{\mathrm{TP}+\mathrm{TN}}{\mathrm{TP}+\mathrm{FP}+\mathrm{TN}+\mathrm{FN}} \times 100 \tag{20}$$

$$P = \frac{\mathrm{TP}}{\mathrm{TP}+\mathrm{FP}} \tag{21}$$

$$F-\mathrm{measure} = \frac{2 \times P \times S_e}{P + S_e} \tag{22}$$

$$\mathrm{MCC} = \frac{\mathrm{TP}\times\mathrm{TN} - \mathrm{FP}\times\mathrm{FN}}{\sqrt{(\mathrm{TP}+\mathrm{FP})\times(\mathrm{TP}+\mathrm{FN})\times(\mathrm{TN}+\mathrm{FP})\times(\mathrm{TN}+\mathrm{FN})}} \tag{23}$$

where n stands for number of data, M_i stands for recorded target value, E_i refers for estimated target value, $\dot{M}$ refers for average of recorded target values, $\dot{E}$ stands for average of estimated target values, S_E refers for total estimated target values, and S_M stands for total recorded target values. Herein, evaluation of the estimation model was done by correlation coefficients (R) according to the basics demonstrated by Colton (1974) which explains if the correlation coefficients were between 0–0.25, 0.25–0.50, 0.50–0.75, and 0.75–1 it indicates there is no-correlation, moderate correlation, high correlation, and perfect correlation, respectively. The values of TP, FP, TN, and FN refers to the number of TPs, false positive, true negatives, and false negatives, respectively. The correlation coefficient and accuracy were evaluated by the goodness of the estimation (Colton, 1974). The accuracy of between 0–0.25, 0.25–0.50, 0.50–0.75, and 0.75–1.0 indicate "little – no relationship", "fair relationship", "moderate – good relationship", and "very good – excellent relationship", respectively.

ROC charts can picture the relationship of the correct estimations of the positive and negative values. This curve graphically shows the rates of TP against the false positive, as its threshold of discrimination is changed. In fact, a model with a particular relationship between TP rate and the false positive rate displays each point on the curve. To better presentation of the information of the ROC curve the values need be assembled into a sole output value in order to make a better comparison between the response of multiple models with statistical criteria (Stegmayer et al., 2013). The total area under the ROC curve is interpreted as an indicator of the system's performance and to

make easy comparison between classifiers it was between 0 and 1 (Bradley, 1997). The values close to 1 indicate that a grade higher than any non-class sample has been assigned to most of the positive class samples, which shows there is a threshold that ideally distinguishes.

3 | RESULTS AND DISCUSSIONS

3.1 | Moisture content and moisture ratio

Figure 2 describes the changes in the moisture content (A) and the moisture ratio (B) for various methods of drying apricot samples. As can be seen, in all the methods, with the passage of time, the moisture content and moisture ratio decreased continuously. When microwaves were used either singly or in combination with other methods, it resulted in the most effect on the drying kinetics. In individual methods like convective and infrared, heat is transferred from the outer surface of the product through conduction, and over time, heat transfer slows down and causes a noteworthy raise in drying time due to the phenomenon of surface hardening and shrinkage (Minaei et al., 2012). Moreover, the maximum amount of moisture removal was obtained for microwave (under different powers) and MW-CV methods. Because in these methods, the airflow speed for apricot samples is due to the internal (volumetric) heat emitted by microwaves. It causes a faster sample dehydration, and as a result, the moisture reaches minimum value quickly (Zhu et al., 2022). Similar findings were found in published studies (EL-Mesery & El-khawaga, 2022; Łechtanska et al., 2015; Roknul Azam et al., 2019; Witrowa-Rajchert & Rząca, 2009).

3.2 | Effective moisture diffusivity

Table 2 exhibits the results of ANOVA analysis of different dryers under different conditions for two variables, D_{eff} and SEC. For each parameter, sum of squares, mean square, F, and significance (Sig.) were calculated. While the F value was 49.769 for D_{eff}, it was 460.255 for SEC. Herein, the power of variation of SEC between applications was revealed.

Based on Figure 3, the lowest D_{eff} was observed in the CV technique at the temperature of 50°C. From the D_{eff} data displayed in Figure 3, it could be found that the apricot sample dried under various drying techniques (CV, IR, MW, MW-CV, and IR-CV) which shows a

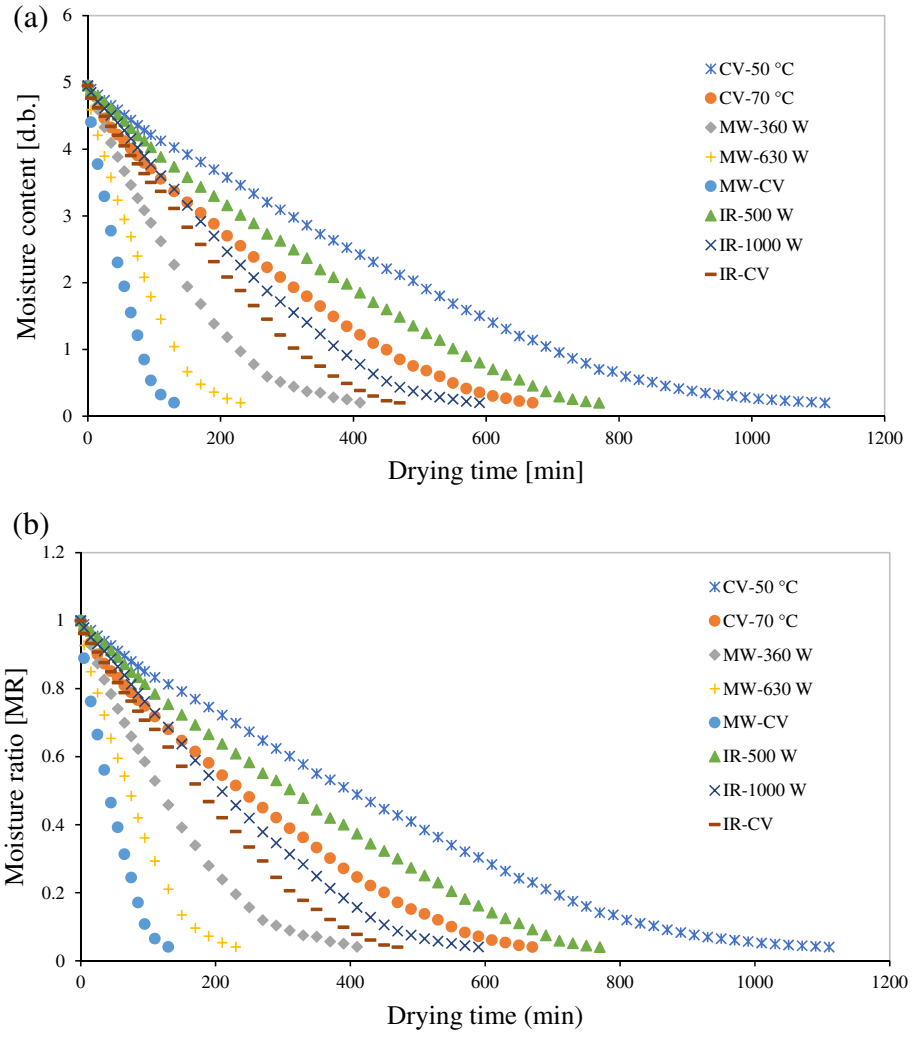

FIGURE 2 Moisture content (a) and moisture ratio (b) versus drying time of apricot sample in different drying methods.

Parameter	Sum of squares	Mean square	F	Sig.
D_{eff}	1.569E-19	2.241E-20	49.769	0.000
Specific energy consumption	95395.125	13627.875	460.255	0.000

TABLE 2 ANOVA analysis results of the D_{eff} and specific energy consumption at different drying methods.

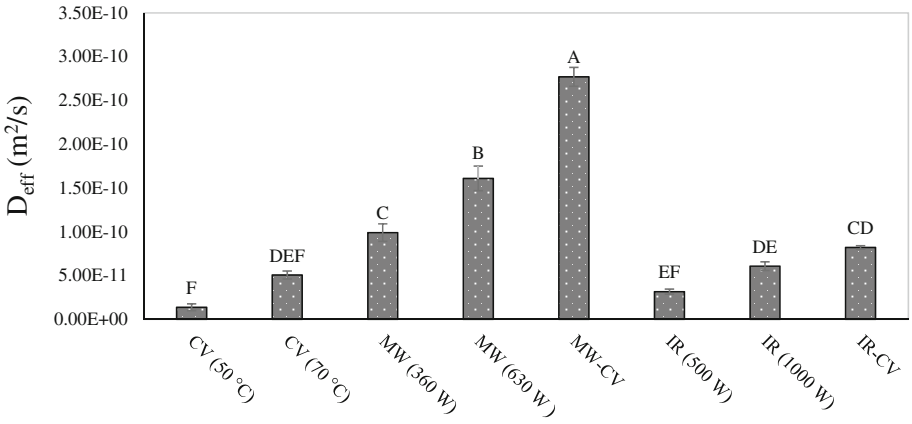

FIGURE 3 Results effects of the different dryers for the D_{eff} at different levels.

certain trend: MW-CV > MW (630 W) > MW (360 W) > IR-CV > IR (750 W) > CV (70°C) > IR (500 W) > CV (50°C). Since there is a direct relationship between the D_{eff} and temperature, on the other hand, the energy of CV to remove moisture is low compared to radiation methods. Therefore, in this method the D_{eff} is at its lowest value compared to other techniques. This finding was in agreement with the result of the study conducted by Behera and Sutar (2018). In the case of the IR method and IR-CV combination, the amount of D_{eff} depends on the power of the infrared lamp leading faster heating of the samples (EL-Mesery et al., 2022). Although the D_{eff} in these methods was higher than the CV method, but it was lower compared to the methods in which microwave energy is used for drying as observed by Bozkir et al. (2021) and Zhu et al. (2022). It can also be seen that the methods in which MW energy was used either individually or in combination with the HA method (MW-CV) for drying, a significant increase in the D_{eff} was observed. Due to the MW power creates internal steam pressure creates a porous structure and greater permeability to steam and finally raises the D_{eff} due to the fast heating of apricot samples (Çetin, 2022c). The highest value of the D_{eff} was obtained in the MW-CV dryer. Similar findings were reported by Çetin (2022c), Simsek and Süfer (2021), and Zhu et al. (2022).

3.3 | Specific energy consumption

According to the results shown in Figure 4, it can be stated that there is no significant difference in the final energy consumption between the 360 W microwave method and the infrared-convective method. But the rest of the drying methods have a significant difference in terms of energy consumption at a statistical level of 5%. In addition, according to Figure 4, the most energy consumption was recorded in the single CV method at a temperature of 50°C. More specifically, in this method, a large share of the energy used for drying was wasted Also, low temperature at drying processes will increase the drying time and consequently increase the energy consumption (Motevali et al., 2014). Similar findings were reported previously (EL-Mesery & El-khawaga, 2022; Łechtanska et al., 2015).

In the infrared method (single and combined with CV), all the energy emitted by the lamps is absorbed by the sample and causes it to heat up causing the product lose moisture faster than the CV method and require less energy (Onwude et al., 2018). Similar outcomes have previously obtained by (Jeevarathinam et al., 2022; Ye et al., 2021).

The lowest energy consumption is recorded for the methods that use microwave power. One of the powerfulness of this method is the high thermal conductivity compared to other methods (convective and infrared power) causing drying time reduction and consequently decreasing energy consumption (Ren et al., 2022). This is due to the vibration of water molecules due to the absorption of microwaves, which covers the entire samples of the product. Motevali and Tabatabaei (2017) performed drying dog-rose with different methods (CV, IR, IR-CV, hybrid photovoltaic/thermal, MW, MW-CV, and vacuum) and in addition, Łechtanska et al. (2015) conducted a study on drying green pepper with using several methods (CV, MW-CV, MW-CV + $IR_{pretreatment}$, and CV + $MW_{pretreatment}$ + $IR_{pretreatment}$, CV + $IR_{pretreatment}$ dryers) and disclosed that the minimum energy consumption value was obtained for microwave dryers similarly to the findings of the present investigation. This result is compatible with the findings of EL-Mesery and El-khawaga (2022), and Motevali et al. (2020).

3.4 | Estimation of drying characteristics

3.4.1 | Moisture content

In the estimation of moisture content, several parameters were employed including drying method, drying time, drying rate, and moisture ratio.

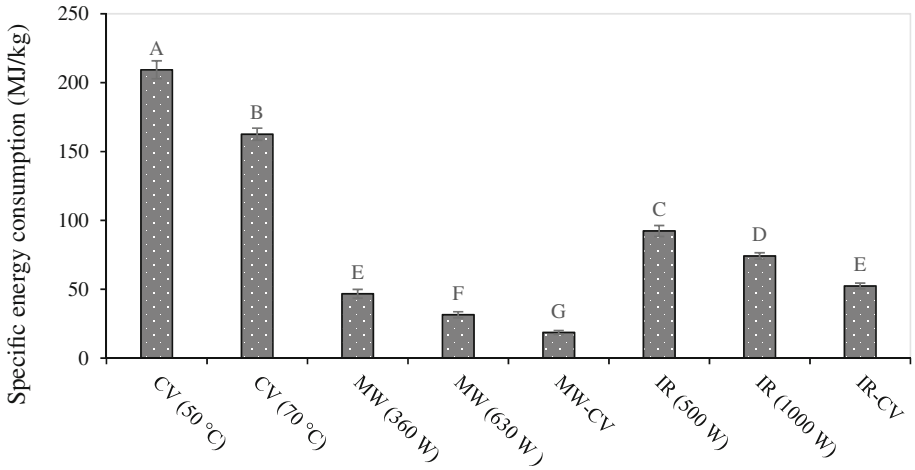

FIGURE 4 Specific energy consumption during the different drying of apricots.

TABLE 3 Performance outcomes of machine learning algorithms in estimation of moisture content.

k-fold cross validation					
Algorithms	***R***	**MAE**	**RMSE**	**RAE (%)**	**RRSE (%)**
MLP (3-3-1)	0.9456	0.3083	0.5225	21.90	33.03
MLP (3-6-1)	0.9622	0.2646	0.4299	18.80	27.18
MLP (3-9-1)	0.9592	0.2840	0.4482	20.18	28.33
GP	0.8949	0.5425	0.7162	38.54	45.27
SVR	0.9733	0.1022	0.3673	7.26	23.22
1-NN	0.9515	0.2231	0.4902	15.85	30.98
3-NN	0.9489	0.2014	0.5030	14.31	31.80
5-NN	0.9460	0.2293	0.5184	16.29	32.77
RF	0.9908	0.1585	0.2372	11.26	14.99
Train-test split					
Algorithms	***R***	**MAE**	**RMSE**	**RAE (%)**	**RRSE (%)**
MLP (3-3-1)	0.9317	0.4781	0.6921	32.49	41.75
MLP (3-6-1)	0.8895	0.6684	0.8257	45.41	49.81
MLP (3-9-1)	0.9252	0.5068	0.6930	34.44	41.80
GP	0.8924	0.5759	0.7810	39.13	47.11
SVR	0.9648	0.1366	0.4465	9.28	26.93
1-NN	0.9370	0.2533	0.5982	17.21	36.09
3-NN	0.9228	0.2684	0.6461	18.23	38.97
5-NN	0.9269	0.2871	0.6260	19.51	37.76
RF	0.9912	0.1824	0.2678	12.39	16.15

Note: MLP-type ANN parameters; η: learning ratio: 0.3; α: momentum coefficient: 0.2; NoE: number of epochs: 500; activation function: sigmoid. The number of inputs is 4, the number of outputs is 1, and the number of neurons in the hidden layers is 4, 8, and 12, respectively.
Abbreviations: AN, artificial neural network; GP, Gaussian processes; KNN, k-nearest neighbors; MAE, mean absolute error; MLP, multilayer perceptron; RAE, relative absolute error; RF, random forest; RMSE, root mean square error; RRSE, root relative squared error; SVR, support vector regression.

The performances of the models suggested for estimation of moisture content of apricot are illustrated in Table 3. The best correlation coefficient (0.9908 and 0.9912) and lowest RMSE (0.2372 and 0.2678) were obtained for RF algorithm using the k-fold cross validation and train-test split method. RF model was followed by the SVR with an *R* of 0.9733 and 0.9648. The lowest *R* values were found by GP and MLP (3-6-1) algorithms with the values of 0.8949 for k-fold and 0.8895 for train-test split. For both methods, the lowest MAE values were obtained from SVR (0.1022 and 0.1366) algorithm. Furthermore, the highest MAE was determined as 0.5425 from GP for

k-fold, 0.6684 from MLP (3-6-1) for train-test split. Additionally, the greatest RAE and RRSE values were found in GP for k-fold and MLP (3-6-1) for train-test split.

In the k-fold cross validation technique, in terms of MLP model performances, the MLP with the structure of 3-6-1 was more successful than the other MLP structures with the *R* value of 0.9622. Moreover, RMSE, RRSE, MAE, and RAE values were lower for this structure. In the present study, for the k-NN, the best *k* value was selected as 1 with the greatest *R* (0.9515) and lowest RMSE (0.4902) values.

In the train-test split method, the most successful MLP structure was 3-3-1. This model recorded the maximum *R*-value by 0.9317 and the minimum MAE and RMSE values by 0.4781 and 0.6921, respectively. In the present investigation, 1-NN showed the maximum *R* (0.9370) value and the minimum MAE (0.2533) and RMSE (0.5982) values among the k-NN models. Based on what was found, the powerful algorithm for the estimation of moisture content was RF both k-fold cross validation and train-test split. The focus was to highlight differences among the algorithms and the variations between the models based on different variables. Herein, Table 3 clearly presents which models and variables are successful in achieving this for the estimation of moisture content.

Comply with the findings of this study; Sağlam and Çetin (2022) reported that for the estimation of moisture content of apple slices, *R*-values were obtained between 0.8728 and 0.9873 for k-NN and RF algorithms, respectively. Kırbaş et al. (2019) found *R* values between 0.09932 and 0.9993 using MLP algorithm for moisture content estimation of pomelo fruit drying. Tarafdar et al. (2019) performed moisture content estimation of mushrooms using ANNs, and the researchers claimed that the greatest *R*-value was 0.9991. Lately, Onu et al. (2022) carried out an investigation for estimation of moisture content of cocoyam samples by R^2 of 0.9583, and 0.9971 for ANN and adaptive neuro-fuzzy inference system (ANFIS) models, respectively. In another study, Rasooli Sharabiani et al. (2021) evaluated the moisture content of apple slices in microwave and convective drying using ANN and they indicated that the *R* values were 0.9991 and 0.9993, respectively. Also, Satorabi et al. (2021) estimated the moisture content of dried apricot samples using ANFIS and genetic algorithm (GA) integrated with ANN (GA-ANN) and obtained the *R* values of 0.9990 for both models.

TABLE 4 Performance outcomes of machine learning algorithms in the estimation of moisture ratio.

***k*-fold cross validation**					
Algorithms	***R***	**MAE**	**RMSE**	**RAE (%)**	**RRSE (%)**
MLP (4-4-1)	0.9999	0.0022	0.0039	0.76	1.22
MLP (4-8-1)	0.9998	0.0028	0.0059	0.98	1.85
MLP (4-12-1)	0.9999	0.0021	0.0037	0.76	1.16
GP	0.9923	0.0325	0.0423	11.42	13.24
SVR	0.9958	0.0076	0.0304	2.66	9.52
1-NN	0.9905	0.0321	0.0452	11.30	14.14
3-NN	0.9910	0.0253	0.0459	8.88	14.36
5-NN	0.9840	0.0301	0.0597	10.57	18.69
RF	0.9996	0.0066	0.0090	2.32	2.81
Train-test split					
Algorithms	***R***	**MAE**	**RMSE**	**RAE (%)**	**RRSE (%)**
MLP (4-4-1)	0.9987	0.0155	0.0216	5.23	6.45
MLP (4-8-1)	0.9985	0.0176	0.0233	5.93	6.97
MLP (4-12-1)	1.0000	0.0013	0.0018	0.44	0.55
GP	0.9893	0.0368	0.0490	12.37	14.62
SVR	0.9958	0.0096	0.0334	3.24	9.97
1-NN	0.9912	0.0333	0.0468	11.21	13.97
3-NN	0.9911	0.0292	0.0474	9.81	14.14
5-NN	0.9851	0.0365	0.0614	12.27	18.33
RF	0.9996	0.0093	0.0121	3.12	3.61

Note: MLP-type ANN parameters; η: learning ratio: 0.3; α: momentum coefficient: 0.2; NoE: number of epochs: 500; activation function: sigmoid. The number of inputs is 4, the number of outputs is 1, and the number of neurons in the hidden layers are 4, 8, and 12, respectively.
Abbreviations: AN, artificial neural network; GP, Gaussian processes; KNN, k-nearest neighbors; MAE, mean absolute error; MLP, multilayer perceptron; RAE, relative absolute error; RF, random forest; RMSE, root mean square error; RRSE, root relative squared error; SVR, support vector regression.

TABLE 5 The mean accuracies and performance metrics for drying methods.

Model *k*-fold cross validation	Acc. (%)	TP rate	Precision	F-measure	MCC	ROC area	PRC area
MLP							
50°C		0.935	0.906	0.921	0.897	0.991	0.983
70°C		0.825	0.943	0.880	0.863	0.974	0.935
360 W		0.852	0.920	0.885	0.873	0.970	0.893
630 W		0.778	0.875	0.824	0.813	0.978	0.901
540 W-60°C	82	0.538	0.778	0.636	0.633	0.918	0.754
500 W		0.933	0.646	0.764	0.725	0.979	0.903
1000 W		0.667	0.828	0.738	0.709	0.925	0.810
500 W-60°C		0.700	0.750	0.724	0.692	0.916	0.695
RF							
50°C		0.935	0.906	0.921	0.897	0.981	0.964
70°C		0.900	0.878	0.889	0.869	0.968	0.922
360 W		0.778	0.808	0.792	0.770	0.957	0.833
630 W		0.667	0.800	0.727	0.713	0.908	0.689
540 W-60°C	78	0.538	1.000	0.700	0.725	0.887	0.698
500 W		0.867	0.848	0.857	0.828	0.969	0.936
1000 W		0.667	0.545	0.600	0.535	0.900	0.528
500 W-60°C		0.467	0.500	0.483	0.421	0.840	0.408
k-NN							
50°C		0.984	0.871	0.924	0.903	0.981	0.966
70°C		0.950	0.792	0.950	0.842	0.964	0.880
360 W		0.778	0.568	0.778	0.621	0.901	0.554
630 W		0.222	0.333	0.222	0.231	0.820	0.366
540 W-60°C	70	0.011	0.100	0.011	0.014	0.816	0.485
500 W		0.889	0.769	0.825	0.790	0.961	0.875
1000 W		0.583	0.512	0.545	0.472	0.825	0.416
500 W-60°C		0.133	0.400	0.200	0.180	0.749	0.235
Model **Train-test split**	**Acc. (%)**	**TP rate**	**Precision**	**F-measure**	**MCC**	**ROC area**	**PRC area**
MLP							
50°C		0.960	0.960	0.960	0.942	1.000	1.000
70°C		0.889	0.800	0.842	0.823	0.900	0.902
360 W		0.875	1.000	0.933	0.929	0.952	0.901
630 W		0.500	0.667	0.571	0.559	0.844	0.577
540 W-60°C	86	0.667	1.000	0.800	0.811	1.000	1.000
500 W		0.933	0.636	0.757	0.709	0.984	0.943
1000 W		0.500	1.000	0.667	0.683	0.968	0.906
500 W-60°C		1.000	1.000	1.000	1.000	1.000	1.000
RF							
50°C		0.920	1.000	0.958	0.942	0.996	0.992
70°C		0.889	0.727	0.800	0.777	0.905	0.854
360 W		0.750	1.000	0.857	0.854	0.889	0.825
630 W		0.500	0.667	0.571	0.559	0.659	0.441
540 W-60°C	77	0.667	0.286	0.400	0.405	0.966	0.758
500 W		0.800	0.923	0.857	0.831	0.945	0.889

(Continues)

TABLE 5 (Continued)

Model / Train-test split	Acc. (%)	TP rate	Precision	F-measure	MCC	ROC area	PRC area
1000 W		0.500	0.500	0.500	0.430	0.837	0.578
500 W-60°C		0.571	0.500	0.533	0.487	0.862	0.360
k-NN							
50°C		1.000	0.833	0.909	0.871	0.998	0.993
70°C		0.889	0.800	0.842	0.823	0.934	0.782
360 W		0.750	0.545	0.632	0.594	0.908	0.568
630 W		0.250	0.500	0.333	0.331	0.607	0.162
540 W-60°C	71	0.333	1.000	0.500	0.570	0.641	0.358
500 W		0.800	0.706	0.750	0.691	0.899	0.699
1000 W		0.300	0.429	0.353	0.285	0.665	0.297
500 W-60°C		0.143	0.333	0.200	0.172	0.778	0.203

Abbreviations: k-NN, k-nearest neighbor; MCC, Matthews correlation coefficient; MLP, multilayer perceptron; PRC, precision–recall; RF, random forest; ROC, receiver operating characteristic; TP, true positive.

3.4.2 | Moisture ratio

Table 4 exhibits the performance findings of the estimation of moisture ratio. In the k-fold cross validation, the best *R*-values were calculated for MLP (4-4-1) and MLP (4-12-1) algorithms with a value of 0.9999. The least MAE (0.0021) and RMSE (0.0059) were found for MLP (4-12-1) model. The 5-NN had the lowest *R* as 0.9840, and the SVR had highest MAE and RAE as 0.0325 and 11.42%, respectively. Among the k-NN models, the most successful one was the 3-NN due to the greatest *R* (0.9910) and the minimum MAE (0.0253) and RAE (8.88%). In the test-train split method, the best correlation coefficient obtained for MLP (4-12-1) with the value of 1.0000, and this was also the best result of the present study. More specifically, the MLP model (4-12-1) presented the minimum MAE (0.0013), RMSE (0.0018), RAE (0.44%), and RRSE (0.55%). This algorithm was developed with the *R*-value and RMSE value of 0.9996 and 0.0121, respectively. While the minimum *R*-value of 0.9851 and the highest RMSE value of 0.0614 were found for 5-NN model. In addition, GP and 5-NN had maximum RAE and RRSE percent. In this study, the powerful classifiers for estimation of moisture ratio were MLP models both k-fold cross validation and train-test data groups. Herein, Table 4 shows the success of MLP and RF models for the estimation of moisture content. It has been proven that variations in MLP structure could positively increment the results.

Different models were applied to drying characteristics in previous studies, and similar results were obtained in the current study. By using MLP, k-NN, RF, GP, and SVR algorithms Sağlam and Çetin (2022) estimated the moisture ratio of apple slices using six various drying approaches. The best *R* values were reported as 0.9800, 0.9873, and 0.9841 for Golden Delicious, Oregon Spur, and Granny Smith, respectively. Çetin (2022a) estimated moisture ratio using RF, MLP, GP, SVR, and k-NN, and k-NN was an outstanding algorithm with the *R* values of 0.9898 and 0.9942 for Valencia and Washington Navel orange cultivars, respectively. Zadhossein et al. (2022) obtained the greatest R^2 for the estimation of moisture ratio for ANN and ANFIS models as 0.9940 and 0.9978, respectively. Kırbaş et al. (2019) used drying duration, drying method, and thickness of dried sample as the input values to estimate the moisture ratio of pomelo fruit using MLP algorithm, and the *R*-values were from 0.0993 to 0.9931. Taraf-dar et al. (2019) determined the moisture ratio of dried mushrooms using ANNs. Initial and final temperature, process duration, primary moisture content, pressure, and thickness of dried sample were employed as inputs. The best correlation coefficient was found to be 0.9994. Okonkwo et al. (2022) indicated that ANFIS presented better results compared to ANNs for the estimation of moisture values of orange-fleshed sweet potato with correlation coefficient and RMSE values of 0.99786 and 0.0225, respectively. In earlier research, the estimation of moisture ratio of *Echium amoenum* was carried out using ANFIS and ANN by Chasiotis et al. (2021). The ANFIS and ANN models achieved in the study showed the best performance with R^2 values of 0.9992 and 0.9988, respectively. These results also conform to the current study.

3.5 | Discrimination performance results

During current study, dried apricot was discriminated for different drying methods. In the discrimination, moisture content, moisture ratio, drying rate, drying time, and ln (MR) values were used and three different models (MLP, RF, and k-NN) were applied. In case of the model based on drying characteristics of apricots, very good discrimination accuracies were found for all three classifiers.

The mean accuracies and performance metrics for drying methods are presented in Table 5. The MLP generated the greatest accuracy of 82.00%. In addition, RF allowed the drying methods to be discriminated with the accuracy of 78.00%. With the k-NN, the lowest

TABLE 6 Confusion matrix of discriminators for drying methods.

***k*-fold cross validation**								
MLP	50°C	70°C	360 W	630 W	540 W-60°C	500 W	1000 W	540 W-60°C
50°C	58	1	0	0	0	3	0	0
70°C	2	33	0	0	1	3	1	0
360 W	0	0	23	0	0	3	0	1
630 W	0	0	1	14	1	2	0	0
540 W-60°C	0	1	0	2	7	2	0	1
500 W	3	0	0	0	0	42	0	0
1000 W	0	0	1	0	0	6	24	5
500 W-60°C	1	0	0	0	0	4	4	21
RF	50°C	70°C	360 W	630 W	540 W-60°C	500 W	1000 W	540 W-60°C
50°C	58	2	1	0	0	0	0	1
70°C	2	36	0	0	0	1	1	0
360 W	1	0	21	0	0	1	0	4
630 W	1	1	3	12	0	0	1	0
540 W-60°C	0	2	0	3	7	1	0	0
500 W	1	0	0	0	0	39	4	1
1000 W	0	0	1	0	0	3	24	8
500 W-60°C	1	0	0	0	0	1	14	14
k-NN	50°C	70°C	360 W	630 W	540 W-60°C	500 W	1000 W	540 W-60°C
50°C	61	1	0	0	0	0	0	0
70°C	1	38	0	0	0	1	0	0
360 W	2	0	21	0	0	0	1	3
630 W	2	1	10	4	1	0	0	0
540 W-60°C	1	4	0	8	0	0	0	0
500 W	0	3	0	0	0	40	2	0
1000 W	1	1	1	0	0	9	21	3
500 W-60°C	2	0	5	0	0	2	17	4
Test-train split								
MLP	50°C	70°C	360 W	630 W	540 W-60°C	500 W	1000 W	540 W-60°C
50°C	24	1	0	0	0	0	0	0
70°C	0	8	0	0	0	1	0	0
360 W	0	0	7	0	0	1	0	0
630 W	0	1	0	2	1	0	0	0
540 W-60°C	0	0	0	1	2	0	0	0
500 W	1	0	0	0	0	14	0	0
1000 W	0	0	0	0	0	5	5	0
500 W-60°C	0	0	0	0	0	0	0	7
RF	50°C	70°C	360 W	630 W	540 W-60°C	500 W	1000 W	540 W-60°C
50°C	23	2	0	0	0	0	0	0
70°C	0	8	0	0	1	0	0	0
360 W	0	0	6	0	1	0	0	1
630 W	0	1	0	2	1	0	0	0
540 W- 60°C	0	0	0	1	2	0	0	0
500 W	0	0	0	0	1	12	2	0
1000 W	0	0	0	0	1	1	5	3
500 W-60°C	0	0	0	0	0	0	3	4

(Continues)

TABLE 6 (Continued)

Test-train split								
k-NN	50°C	70°C	360 W	630 W	540 W-60°C	500 W	1000 W	540 W-60°C
50°C	25	0	0	0	0	0	0	0
70°C	1	8	0	0	0	0	0	0
360 W	1	0	6	0	0	0	0	1
630 W	1	1	1	1	0	0	0	0
540 W-60°C	0	1	0	1	1	0	0	0
500 W	1	0	0	0	0	12	2	0
1000 W	1	0	0	0	0	5	3	1
500 W-60°C	0	0	4	0	0	0	2	1

Note: Since the values obtained for the drying conditions in the confusion matrices are not the same number, the numbers in the distribution may vary. Color shades represent true positive values.
Abbreviations: k-NN, k-nearest neighbor; MLP, multilayer perceptron; RF, random forest.

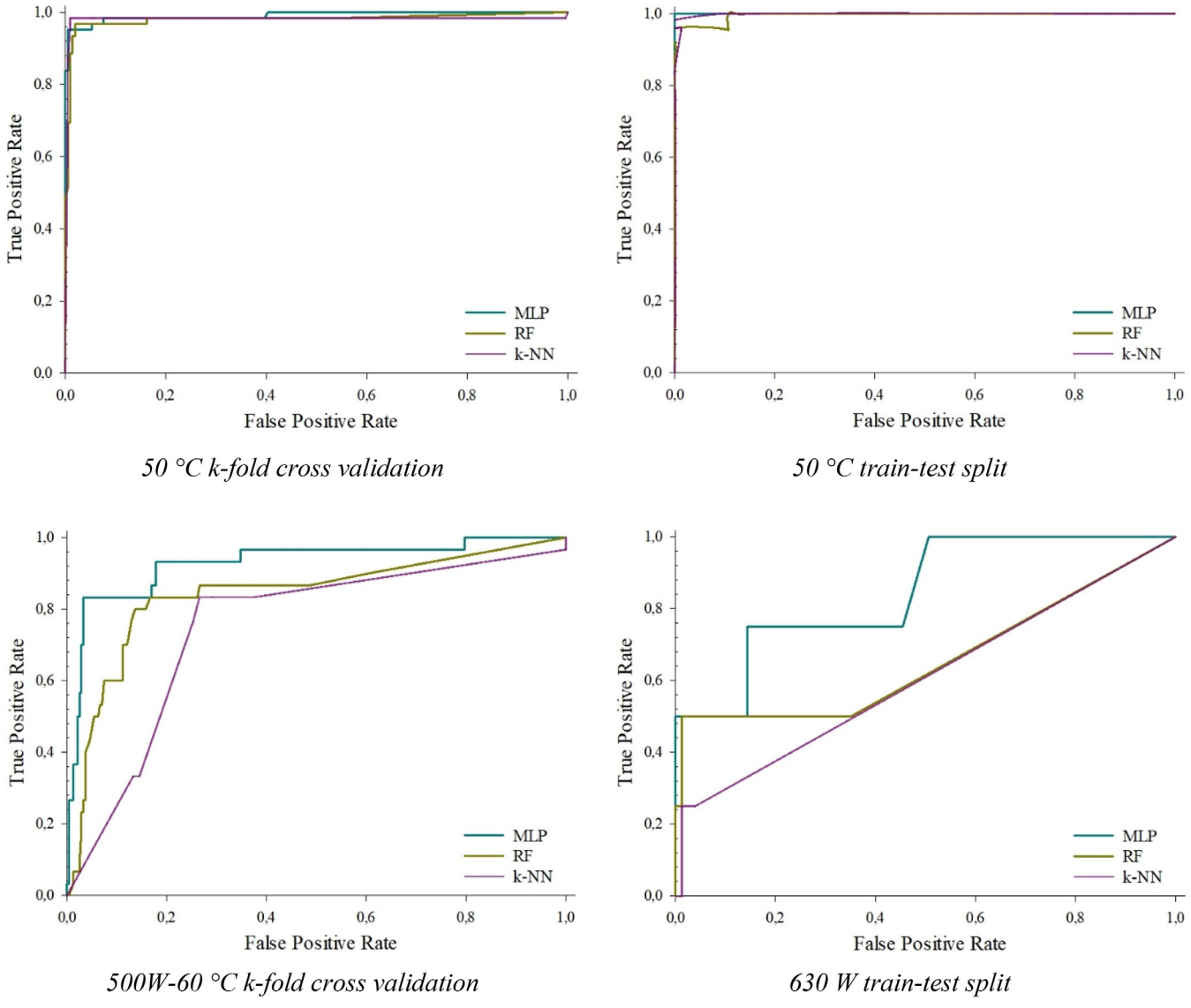

FIGURE 5 The receiver operating characteristic curves of best (above) and worst (bottom) discrimination for developed machine learning algorithms based on drying characteristics.

accuracy was obtained by 70.00%. Additionally, the results of other discrimination metrics supported these findings. With the MLP algorithm, the greatest TP rate amounted to 0.935, F-measure to 0.921, MCC to 0.897, and ROC area to 0.991 at 50°C. The lowest values of TP rate, F-measure, and MCC were found at 540 W and 60°C in k-NN model by 0.011, 0.0.11, and 0.014, respectively. Generally, the lowest ROC area and PRC area values were obtained for 500 W-60°C drying conditions.

Confusion matrix of discriminators for drying methods is given in Table 6. The confusion matrix showed that among 62 50°C air-convective conditions, 58, 58, and 61 were categorized precisely, for MLP, RF, and k-NN respectively. In the train test split method, the greatest accuracy value was determined as 86.00% in MLP algorithm. This algorithm was followed by RF and k-NN with accuracy values of 77.00% and 71.00%, respectively. For the 500 W-60°C hybrid condition, the best TP rate, precision, F-measure, MCC, ROC area, and PRC area values were determined in MLP, while the lowest performance metrics were found with k-NN. Considering these metrices, the highest results were found at 50°C air-convective condition (Table 6). The confusion matrix showed that among 25 values at 50°C air-convective conditions, 24, 23, and 25 were categorized precisely, for MLP, RF, and k-NN, respectively (Table 6).

Researchers have discriminated drying conditions in previous studies according to different drying characteristics. Kurtulmuş et al. (2014) reported the texture feature-based discrimination accuracy of SVM, k-NN, DT, NB, and ANN algorithms for dried tarhana under different conditions by 93.50%, 99.50%, 92.10%, 94.40%, and 98.60% and for step-by-step discriminant assessment-based classifier, by 95.40%, 96.30%, 93.10%, 92.60%, and 91.70% for principal component analysis-based classifier, respectively. Przybył et al. (2020) developed various ANN models for dried strawberry sorting using acoustic technique and reported RMSE values of 0.16, 0.09, and 0.35 for MLP structures of (2-6-1), (2-14-1), and (2-4-1), respectively. Makarichian et al. (2021) evaluated various drying methods for garlic as fluid bed dryer with in-line near-infrared, atmospheric freeze-drying, and vacuum dryer with near-infrared techniques. The authors obtained accuracy values of 96.67% for linear discriminant analysis and 100% for backpropagation neural network (BPNN). Lately, Ropelewska and Wrzodak (2022) implied that the distinction exactness of freeze-dried beetroot using textural characteristics was from 85% to 96% for RF, logistic, and PART algorithms.

ROC area curves showed that drying methods for all classifiers were established based on drying characteristics. The receiver-operating curve represents the performance of the classifiers that approved that this classifier precisely recognized drying methods. Expectedly the highest ROC area values were found for MLP algorithm. Particularly, the ROC area values certify very high performance for automatic identification of any understudy of the drying method discrimination. As seen in the ROC area curves (Figure 5), the best discriminated method was 50°C convective drying of both k-fold cross validation and train-test split while the worst discriminated methods were 500 W-60°C k-fold cross validation and 630 W train-test split.

4 | CONCLUSIONS

Drying characteristics of the apricots should be optimized for designing the related dryers and quality assessment. Present findings show that the drying characteristics and product-related features could differ between methods and therefore machine learning approaches could be employed as a functional technique for discrimination as well as for the development of precision drying systems. Among algorithms, the RF and MLP are found as optimum classifiers for estimation and discrimination. The highest and lowest amount of drying time and SEC were obtained in CV and MW-CV dryers, respectively.

In this study, the main challenge was the absence of image processing techniques during estimation and classification. The accuracy of the estimations could have been improved if image analysis had been used to obtain information about the size, shape, and color of the product. Additionally, it would have allowed us to obtain results more rapidly. The current procedure applying machine learning to drying characteristics may have great practical application in apricot drying processes. Models based on moisture content and moisture ratio have been shown to be an effective method for monitoring, controlling, and optimizing drying systems. The estimation models proposed in this study provide useful information for the development of sustainable and smart technologies in similar products. In addition, for future research, it is suggested to perform a supplementary examination to find out the influences of other drying characteristics such as drying temperature, microwave, and infrared power using new machine learning approaches. In addition, it would be beneficial to test deep learning algorithms supported by image processing and develop new models. This could enhance the efficiency of measurements and overall performance results.

AUTHOR CONTRIBUTIONS

Mohammad Kaveh: Conceptualization; methodology; formal analysis; computation and writing. **Necati Çetin**: Software; visualization; validation; data curation and writing. **Esmail Khalife**: Formal analysis; investigation; writing and editing. **Yosef Abbaspour-Gilandeh**: Conceptualization; investigation; writing and editing. **Maryam Sabouri**: Formal analysis and writing. **Faroogh Sharifian**: Investigation and writing.

FUNDING INFORMATION

No funding was received for this study.

CONFLICT OF INTEREST STATEMENT

The authors declare no conflicts of interest.

DATA AVAILABILITY STATEMENT

All the data used in the manuscript are available in the tables and figures. The data that support the findings of this study are available from the corresponding author upon reasonable request.

ORCID

Mohammad Kaveh https://orcid.org/0000-0001-5285-2211
Necati Çetin https://orcid.org/0000-0001-8524-8272
Esmail Khalife https://orcid.org/0000-0002-1690-1714
Yousef Abbaspour-Gilandeh https://orcid.org/0000-0002-9999-7845
Faroogh Sharifian https://orcid.org/0000-0003-1804-7344

REFERENCES

Abbasi, S. A., Sharifzadeh, F., Tavakol, A. R., Majnoun, H. N., & Gazor, H. (2010). Optimization of process parameters of soybean seeds dried in a constant-bed dryer using response surface methodology. *Journal of Agricultural Science and Technology*, *12*, 409–423.

Afkhamipour, M., Mofarahi, M., Borhani, T. N. G., & Zanganeh, M. (2018). Prediction of heat capacity of amine solutions using artificial neural network and thermodynamic models for CO 2 capture processes. *Heat and Mass Transfer*, *54*, 855–866.

Ali, J., Khan, R., Ahmad, N., & Maqsood, I. (2012). Random forests and decision trees. *International Journal of Computer Science Issues (IJCSI)*, *9*(5), 272.

AOAC. (1990). *Official method of analysis*. Association of Official Analytical Chemists.

Ashtiani, S. H. M., Javanmardi, S., Jahanbanifard, M., Martynenko, A., & Verbeek, F. J. (2021). Detection of mulberry ripeness stages using deep learning models. *IEEE Access*, *9*, 100380–100394.

Bahmani, A., Jafari, S. M., Shahidi, S. A., & Dehnad, D. (2016). Mass transfer kinetics of eggplant during osmotic dehydration by neural networks. *Journal of Food Processing and Preservation*, *40*(5), 815–827.

Bao, X., Min, R., Zhou, K., Traffano-Schiffo, M. V., Dong, Q., & Luo, W. (2023). Effects of vacuum drying assisted with condensation on drying characteristics and quality of apple slices. *Journal of Food Engineering*, *340*, 111286.

Bateni, S. M., Borghei, S. M., & Jeng, D. S. (2007). Neural network and neuro-fuzzy assessments for scour depth around bridge piers. *Engineering Applications of Artificial Intelligence*, *20*(3), 401–414.

Behera, G., & Sutar, P. P. (2018). Effect of convective, infrared and microwave heating on drying rates, mass transfer characteristics, milling quality and microstructure of steam gelatinized Paddy. *Journal of Food Process Engineering*, *41*(8), e12900.

Berhane, T. M., Lane, C. R., Wu, Q., Autrey, B. C., Anenkhonov, O. A., Chepinoga, V. V., & Liu, H. (2018). Decision-tree, rule-based, and random forest classification of high-resolution multispectral imagery for wetland mapping and inventory. *Remote Sensing*, *10*(4), 580.

Bozkir, H., Tekgül, Y., & Erten, E. S. (2021). Effects of tray drying, vacuum infrared drying, and vacuum microwave drying techniques on quality characteristics and aroma profile of orange peels. *Journal of Food Process Engineering*, *44*(1), e13611.

Bradley, A. P. (1997). The use of the area under the ROC curve in the evaluation of machine learning algorithms. *Pattern Recognition*, *30*(7), 1145–1159.

Breiman, L. (2001). Random forests. *Machine Learning*, *45*, 5–32. https://doi.org/10.1023/A:1010933404324

Çetin, N. (2022a). Prediction of moisture ratio and drying rate of orange slices using machine learning approaches. *Journal of Food Processing and Preservation*, *46*(11), e17011.

Çetin, N. (2022b). Machine learning for varietal binary classification of soybean (*Glycine max* (L.) Merrill) seeds based on shape and size attributes. *Food Analytical Methods*, *15*, 2260–2273.

Çetin, N. (2022c). Comparative assessment of energy analysis, drying kinetics, andbiochemical composition of tomato waste under different drying conditions. *Scientia Horticulturae*, *305*, 111405.

Çetin, N., Karaman, K., Beyzi, E., Sağlam, C., & Demirel, B. (2021). Comparative evaluation of some quality characteristics of sunflower oilseeds (*Helianthus annuus* L.) through machine learning classifiers. *Food Analytical Methods*, *14*(8), 1666–1681.

Chasiotis, V., Nadi, F., & Filios, A. (2021). Evaluation of multilayer perceptron neural networks and adaptive neuro-fuzzy inference systems for the mass transfer modeling of *Echium amoenum* Fisch. & CA Mey. *Journal of the Science of Food and Agriculture*, *101*(15), 6514–6524.

Chicco, D., Tötsch, N., & Jurman, G. (2021). The Matthews correlation coefficient (MCC) is more reliable than balanced accuracy, bookmaker informedness, and markedness in two-class confusion matrix evaluation. *Biodata Mining*, *14*(1), 1–22.

Chikpah, S. K., Korese, J. K., Sturm, B., & Hensel, O. (2022). Colour change kinetics of pumpkin (*Cucurbita moschata*) slices during convective air drying and bioactive compounds of the dried products. *Journal of Agriculture and Food Research*, *10*, 100409.

Colton, T. (1974). *Statistics in medicine* (p. 179). Little Brown and Co.

Daliran, A., Taki, M., Marzban, A., Rahnama, M., & Farhadi, R. (2023). Experimental evaluation and modeling the mass and temperature of dried mint in greenhouse solar dryer; application of machine learning method. *Case Studies in Thermal Engineering*, *47*, 103048.

EL-Mesery, H. S., & El-khawaga, S. E. (2022). Drying process on biomass: Evaluation of the drying performance and energy analysis of different dryers. *Case Studies in Thermal Engineering*, *33*, 101953.

EL-Mesery, H. S., Sarpong, F., Xu, W., & Elabd, M. A. (2022). Design of low-energy consumption hybrid dryer: A case study of garlic (*Allium sativum*) drying process. *Case Studies in Thermal Engineering*, *33*, 101929.

Golpour, I., Chayjan, R. A., Parian, J. A., & Khazaei, J. (2018). Prediction of paddy moisture content during thin layer drying using machine vision and artificial neural networks. *Journal of Agricultural Science and Technology*, *17*, 287–298.

Golpour, I., Kaveh, M., Amiri Chayjan, R., & Guiné, R. P. (2020). Optimization of infrared-convective drying of white mulberry fruit using response surface methodology and development of a predictive model through artificial neural network. *International Journal of Fruit Science*, *20*(2), 1015–1035.

Guiné, R. P., Cruz, A. C., & Mendes, M. (2014). Convective drying of apples: Kinetic study, evaluation of mass transfer properties and data analysis using artificial neural networks. *International Journal of Food Engineering*, *10*(2), 281–299.

Hall, M., Frank, E., Holmes, G., Pfahringer, B., Reutemann, P., & Witten, I. H. (2009). The WEKA data mining software: An update. *ACM SIGKDD Explorations Newsletter*, *11*(1), 10–18.

Jahanbakhshi, A., & Salehi, R. (2019). Processing watermelon waste using *Saccharomyces cerevisiae* yeast and the fermentation method for bioethanol production. *Journal of Food Process Engineering*, *42*(7), e13283.

Jeevarathinam, G., Pandiselvam, R., Pandiarajan, T., Preetha, P., Krishnakumar, T., Balakrishnan, M., Thirupathi, V., Ganapathy, S., & Amirtham, D. (2022). Design, development, and drying kinetics of infrared-assisted hot air dryer for turmeric slices. *Journal of Food Process Engineering*, *45*(6), e13876.

Kaveh, M., & Abbaspour-Gilandeh, Y. (2019). Impacts of hybrid (convective-infrared-rotary drum) drying on the quality attributes of green pea. *Journal of Food Process Engineering*, *43*(7), e13424.

Kaveh, M., & Abbaspour-Gilandeh, Y. (2022). Drying characteristics, specific energy consumption, qualitative properties, total phenol compounds, and antioxidant activity during hybrid hot air-microwave-rotary drum drying of green pea. *Iranian Journal of Chemistry and Chemical Engineering*, *41*(2), 652–669.

Kaveh, M., Çetin, N., Gilandeh, Y. A., Sharifian, F., & Szymanek, M. (2023). Comparative evaluation of greenhouse gas emissions and specific energy consumption of different drying techniques in pear slices. *European Food Research and Technology*, 1–15. https://doi.org/10.1007/s00217-023-04346-2

Kayran, S., & Doymaz, I. (2019). Infrared dryıng of aprıcot pomace. *Latin American Applied Research*, *49*(4), 213–218.

Kayran, S., & Doymaz, I. (2021). Drying of cataloglu apricots: The effect of sodium metabisulfite solution on drying kinetics, diffusion coefficient, and color parameters. *International Journal of Fruit Science*, *21*(1), 270–283.

Kırbaş, İ., Tuncer, A. D., Şirin, C., & Usta, H. (2019). Modeling and developing a smart interface for various drying methods of pomelo fruit (*Citrus maxima*) peel using machine learning approaches. *Computers and Electronics in Agriculture*, *165*, 104928.

Kurtulmuş, F., Gürbüz, O., & Değirmencioğlu, N. (2014). Discriminating drying method of tarhana using computer vision. *Journal of Food Process Engineering*, *37*(4), 362–374.

Łechtanska, J. M., Szadzinska, J., & Kowalski, S. J. (2015). Microwave- and infrared-assisted convective drying of green pepper: Quality and energy considerations. *Chemical Engineering and Processing*, *98*, 155–164.

Loan, L. T. K., Thuy, N. M., & Tai, N. V. (2023). Mathematical and artificial neural network modeling of hot air drying kinetics of instant "Cẩm" brown rice. *Food Science and Technology*, *43*, e27623.

Luka, B. S., Yuguda, T. K., Adnouni, M., Zakka, R., Abdulhamid, I. B., & Gargea, B. G. (2022). Drying temperature-dependent profile of bioactive compounds and prediction of antioxidant capacity of cashew apple pomace using coupled Gaussian process regression and support vector regression (GPR–SVR) model. *Heliyon*, *8*(9), e10461.

Makarichian, A., Chayjan, R. A., Ahmadi, E., & Mohtasebi, S. S. (2021). Assessment the influence of different drying methods and pre-storage periods on garlic (*Allium sativum* L.) aroma using electronic nose. *Food and Bioproducts Processing*, *127*, 198–211.

Malakar, S., Dhurve, P., & Arora, V. K. (2023). Modeling and optimization of osmo-sonicated dehydration of garlic slices in a novel infrared dryer using artificial neural network and response surface methodology. *Journal of Food Process Engineering*, *46*(6), e14261.

Maxwell, A. E., Warner, T. A., & Fang, F. (2018). Implementation of machine-learning classification in remote sensing: An applied review. *International Journal of Remote Sensing*, *39*(9), 2784–2817.

Meerasri, J., & Sothornvit, R. (2022). Artificial neural networks (ANNs) and multiple linear regression (MLR) for prediction of moisture content for coated pineapple cubes. *Case Studies in Thermal Engineering*, *33*, 101942.

Minaei, S., Motevali, A., Najafi, G., & Seyedi, S. R. M. (2012). Influence of drying methods on activation energy, effective moisture diffusion and drying rate of pomegranate arils (*Punica Granatum*). *Australian Journal of Crop Science*, *6*(4), 584–591.

Motevali, A., Jafari, H., Molkabadi, E. Z., Zhu, S., Koloor, R. T., & Taghizadeh-Alisaraei, A. (2020). Comparison of environmental pollution and social cost analyses in different drying technologies. *International Journal of Global Warming*, *22*(1), 1–29.

Motevali, A., Minaei, S., Banakar, A., Ghobadian, B., & Khoshtaghaza, M. H. (2014). Comparison of energy parameters in various dryers. *Energy Conversion and Management*, *87*, 711–725.

Motevali, A., Minaei, S., Khoshtaghaza, M. H., & Amirnejat, H. (2011). Comparison of energy consumption and specific energy requirements of different methods for drying mushroom slices. *Energy*, *36*, e6441.

Motevali, A., & Tabatabaei, S. R. (2017). A comparison between pollutants and greenhouse gas emissions from operation of different dryers based on energy consumption of power plants. *Journal of Cleaner Production*, *154*, 445–461.

Movagharnejad, K., & Nikzad, M. (2007). Modeling of tomato drying using artificial neural network. *Computers and Electronics in Agriculture*, *59*(1–2), 78–85.

Namjoo, M., Moradi, M., & Niakousari, M. (2022). Evaluation of the effect of high-power ultrasound waves on conventional air drying of cumin seeds. *Sustainable Energy Technologies and Assessments*, *52*, 102262.

Okonkwo, C. E., Olaniran, A. F., Adeyi, A. J., Adeyi, O., Ojediran, J. O., Erinle, O. C., & Taiwo, A. E. (2022). Neural network and adaptive neuro-fuzzy inference system modeling of the hot air-drying process of orange-fleshed sweet potato. *Journal of Food Processing and Preservation*, *46*(3), e16312.

Onu, C. E., Igbokwe, P. K., Nwabanne, J. T., & Ohale, P. E. (2022). ANFIS, ANN, and RSM modeling of moisture content reduction of cocoyam slices. *Journal of Food Processing and Preservation*, *46*(1), e16032.

Onwude, D. I., Hashim, N., Abdan, K., Janius, R., & Chen, G. (2018). Investigating the influence of novel drying methods on sweet potato (*Ipomoea batatas* L.): Kinetics, energy consumption, color, and microstructure. *Journal of Food Process Engineering*, *41*(4), e12686.

Parker, J. R. (2001). Rank and response combination from confusion matrix data. *Information Fusion*, *2*(2), 113–120.

Peter, M., Liu, Z., Fang, Y., Dou, X., Awuah, E., Soomro, S. A., & Chen, K. (2021). Computational intelligence and mathematical modelling in chanterelle mushrooms' drying process under heat pump dryer. *Biosystems Engineering*, *212*, 143–159.

Polat, A., & Izli, N. (2022). Determination of drying kinetics and quality parameters for drying apricot cubes with electro hydrodynamic, hot air and combined electro hydrodynamic-hot air drying methods. *Drying Technology*, *40*(3), 527–542.

Przybył, K., Duda, A., Koszela, K., Stangierski, J., Polarczyk, M., & Gierz, Ł. (2020). Classification of dried strawberry by the analysis of the acoustic sound with artificial neural networks. *Sensors*, *20*(2), 499.

Rasmussen, C. E., & Williams, C. K. (2006). *Gaussian process for machine learning*. MIT press.

Rasooli Sharabiani, V., Kaveh, M., Abdi, R., Szymanek, M., & Tanaś, W. (2021). Estimation of moisture ratio for apple drying by convective and microwave methods using artificial neural network modeling. *Scientific Reports*, *11*(1), 1–12.

Ren, S., Zheng, E., Zhao, T., Hu, S., & Yang, H. (2022). Evaluation of physicochemical properties, equivalent umami concentration and antioxidant activity of *Coprinus comatus* prepared by different drying methods. *LWT – Food Science and Technology*, *162*(2022), 113479.

Rodríguez, J., Clemente, G., Sanjuán, N., & Bon, J. (2014). Modelling drying kinetics of thyme (*Thymus vulgaris* L.): Theoretical and empirical models, and neural networks. *Food Science and Technology International*, *20*(1), 13–22.

Rodriguez-Galiano, V. F., Ghimire, B., Rogan, J., Chica-Olmo, M., & Rigol-Sanchez, J. P. (2012). An assessment of the effectiveness of a random forest classifier for land-cover classification. *Journal of Photogrammetry and Remote Sensing*, *67*, 93–104.

Roknul Azam, S. M., Zhang, M., Law, C. L., & Mujumdar, A. S. (2019). Effects of drying methods on quality attributes of peach (*Prunus persica*) leather. *Drying Technology*, *37*(3), 341–351.

Romero, J. R., Roncallo, P. F., Akkiraju, P. C., Ponzoni, I., Echenique, V. C., & Carballido, J. A. (2013). Using classification algorithms for predicting durum wheat yield in the province of *Buenos aires*. *Computer and Electronics in Agriculture*, *96*, 173–179.

Ropelewska, E., & Szwejda-Grzybowska, J. (2021). A comparative analysis of the discrimination of pepper (*Capsicum annuum* L.) based on the cross-section and seed textures determined using image processing. *Journal of Food Process Engineering*, *44*(6), e13694.

Ropelewska, E., & Wrzodak, A. (2022). The use of image analysis and sensory analysis for the evaluation of cultivar differentiation of freeze-dried and lacto-fermented beetroot (*Beta vulgaris* L.). *Food Analytical Methods*, *15*(4), 1026–1041.

Sağlam, C., & Çetin, N. (2022). Machine learning algorithms to estimate drying characteristics of apples slices dried with different methods. *Journal of Food Processing and Preservation*, *46*(10), e16496.

Satorabi, M., Salehi, F., & Rasouli, M. (2021). The influence of xanthan and balangu seed gums coats on the kinetics of infrared drying of apricot slices: GA-ANN and ANFIS modeling. *International Journal of Fruit Science*, *21*(1), 468–480.

Shekarchizadeh, H., Tikani, R., & Kadivar, M. (2014). Optimization of cocoa butter analog synthesis variables using neural networks and genetic algorithm. *Journal of Food Science and Technology*, *51*(9), 2099–2105.

Shimpy, M., & Kumar, A. (2023). Performance assessment and modeling techniques for domestic solar dryers. *Food Engineering Reviews*, *15*, 525–547.

Silva, B. G. D., Frattini Fileti, A. M., & Pereira Taranto, O. (2015). Drying of Brazilian pepper-tree fruits (*Schinus terebinthifolius* Raddi): Development of classical models and artificial neural network approach. *Chemical Engineering Communications*, *202*(8), 1089–1097.

Simsek, M., & Süfer, O. (2021). Influence of different pretreatments on hot air and microwave-hot air combined drying of white sweet cherry. *Turkish Journal of Agriculture – Food Science and Technology*, *9*(6), 1172–1179.

Souza, A. U., Correa, J. L. G., Tanikawa, D. H., Abrahao, F. R., Junqueira, J. R. D. J., & Jimenez, E. C. (2022). Hybrid microwave-hot air drying of the osmotically treated carrots. *LWT – Food Science and Technology*, *156*, 113046.

Stegmayer, G., Milone, D. H., Garran, S., & Burdyn, L. (2013). Automatic recognition of quarantine citrus diseases. *Expert Systems with Applications*, *40*(9), 3512–3517.

Tarafdar, A., Shahi, N. C., & Singh, A. (2019). Freeze-drying behaviour prediction of button mushrooms using artificial neural network and comparison with semi-empirical models. *Neural Computing and Applications*, *31*(11), 7257–7268.

Tripathy, S., & Srivastav, P. P. (2023). Effect of dielectric barrier discharge (DBD) cold plasma-activated water pre-treatment on the drying properties, kinetic parameters, and physicochemical and functional properties of *Centella asiatica* leaves. *Chemosphere*, *332*, 138901.

Trivedi, D., Gautam, S. P., Abdul, S., Hazarika, M. K., & Chakraborty, S. (2023). Instant decompression-induced swell drying of banana: Machine learning and swarm intelligence embedded modeling and process optimization. *Journal of Food Process Engineering*, e14431.

Varol, İ. S., Çetin, N., & Kirnak, H. (2022). Evaluation of image processing technique on quality properties of chickpea seeds (*Cicer arietinum* L.) using machine learning algorithms. *Journal of Agricultural Sciences*, *29*(2), 427–442.

Witrowa-Rajchert, D., & Rząca, M. (2009). Effect of drying method on the microstructure and physical properties of dried apples. *Drying Technology*, *27*, 903–909.

Wu, A., Zhu, J., & Ren, T. (2020). Detection of apple defect using laser-induced light backscattering imaging and convolutional neural network. *Computers & Electrical Engineering*, *81*, 106454.

Ye, L., EL-Mesery, H. S., Ashfaq, M. M., Shi, Y., Zicheng, H., & Alshaer, W. G. (2021). Analysis of energy and specific energy requirements in various drying process of mint leaves. *Case Studies in Thermal Engineering*, *26*, 101113.

Zadhossein, S., Abbaspour-Gilandeh, Y., Kaveh, M., Kalantari, D., & Khalife, E. (2022). Comparison of two artificial intelligence methods (ANNs and ANFIS) for estimating the energy and exergy of drying cantaloupe in a hybrid infrared-convective dryer. *Journal of Food Processing and Preservation*, *46*(10), e16836.

Zadhossein, S., Abbaspour-Gilandeh, Y., Kaveh, M., Nadimi, M., & Paliwal, J. (2023). Comparison of the energy and exergy parameters in cantaloupe (*Cucurbita maxima*) drying using hot air. *Smart Agricultural Technology*, *1*(4), 100198.

Zhang, F., Shi, L., Xin, L., Li, L., Tian, L., Cui, X., & Gao, Y. (2022). Study on drying characteristics and moisture content prediction model of Panax notoginseng taproot by using segmented drying of microwave vacuum combined with hot air. *Journal of Food Process Engineering*, *45*(12), e14179.

Zhu, K., Liu, W., Ren, G., Duan, X., Cao, W., Li, L., Qiu, C., & Chu, Q. (2022). Comparative study on the resveratrol extraction rate and antioxidant activity of peanut treated by different drying methods. *Journal of Food Process Engineering*, *45*(4), e14004.

How to cite this article: Kaveh, M., Çetin, N., Khalife, E., Abbaspour-Gilandeh, Y., Sabouri, M., & Sharifian, F. (2023). Machine learning approaches for estimating apricot drying characteristics in various advanced and conventional dryers. *Journal of Food Process Engineering*, *46*(12), e14475. https://doi.org/10.1111/jfpe.14475